

Structure of spiral arms in M 31

P. Tenjes^{1,2}, T. Tuvikene¹, R. Kipper^{1,2}, A. Tamm¹, and E. Tempel¹

¹ Tartu Observatory, Observatooriumi 1, 61602 Tõravere, Estonia

² Institute of Physics, University of Tartu, Riia 142, 51014 Tartu, Estonia
e-mail: peeter.tenjes@ut.ee

Abstract. In addition to optical imaging, the spiral arms of the nearby Andromeda galaxy (M 31) are well resolved in a broad range of emission data: Far- and Near-UV, CO, HI, Far-IR. In the present contribution, emission distribution along spiral arm cross sections in these different datasets are compared to each other, in order to detect possible shifts between the emission distributions as predicted by the density wave theory. Ten segments were selected from the de-projected spiral arms. To reduce noise introduced by the clumpy nature of the spiral arm, emission along the spiral segments was integrated. No systematic shifts between the UV emission and Far-IR/CO emission across the spiral segments was detected in the observational data.

Key words. Galaxies: individual: Andromeda, M 31 – Galaxies: ISM – Galaxies: structure – Galaxies: star formation – Galaxies: spiral

1. Introduction

Spiral structure of M31 can be approximated by two logarithmic spirals predicted by the density wave theory (e.g. Gordon et al. 2006; Hu et al. 2013). These spirals are not continuous but consist of several segments (see also Efremov 2009). In addition, a circular ring have been added to logarithmic spirals. If quasi-stationary density waves are responsible for spiral arm formation, then offsets between the distributions of different star formation tracers across the spiral arms should be seen. Deriving offsets as a function of galactocentric radius the pattern speed of spirals can be calculated (Egusa et al. 2004; Louie et al. 2013). Strongest differences in distributions of different star formation tracers can be expected when comparing molecular gas/dust densities and emission from very young stars.

On the other hand, if spiral arms are formed due to density inhomogenities there are no offsets or they are small and they do not have regular distribution (Grand et al. 2012a,b; D’Onghia et al. 2013).

2. Aims and methods

In addition to optical imaging (Tempel et al. 2011), the spiral arms of the Andromeda galaxy are well resolved in a broad range of emission data: near- and far-ultraviolet (Thilker et al. 2005), CO (Nieten et al. 2006), HI (Corbelli et al. 2010), near-infrared (Barmby et al. 2006), far-infrared (Fritz et al. 2012).

The aim of the present study is to compare to each other cross sections of emission distributions from all these different star formation tracers along spiral arms. Ten segments were

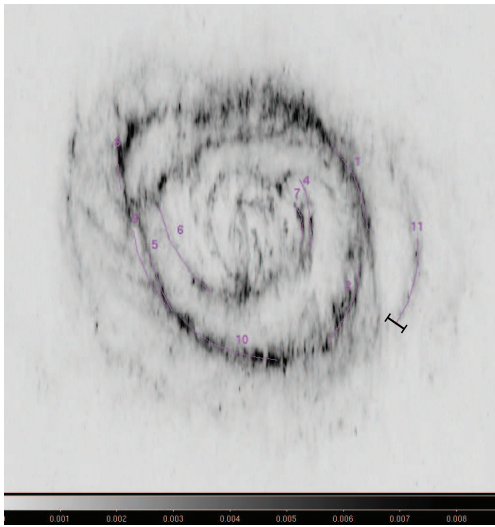


Fig. 1. De-projected far-infrared emission map of M 31 and selected segments. Segments 4, 8 and 9 were selected on the basis of near-ultraviolet maps. Emission along segments were integrated giving us cross sections (profiles) of segments. Width of cross sections is the same for all segments and is indicated for the segment 11.

selected visually from the de-projected images of M 31 (Fig. 1). Segments 1, 2, 5, 6, 7, 10 and 11 were selected on the basis of Herschel far-infrared (FIR) emission, segments 4, 8 and 9 were selected on the basis of GALEX near-ultraviolet (NUV) emission distribution. To reduce noise introduced by the clumpy nature of spiral arms, emission along these segments were integrated giving us cross sections (profiles) of segments. NUV emission maps were corrected from dust absorption in M 31 according to our extinction model (Tempel et al. 2010). As an illustration extinction corrected and uncorrected emission Galex NUV emission distribution cross sections for segments 1 and 10 are given in Fig. 2.

Emission profiles for segment 10 (Fig. 4) have also well defined peaks without any offset between them. NUV emission profile of segment 2 is quite messy. Significant amount of young stars is in the inner side of the segment.

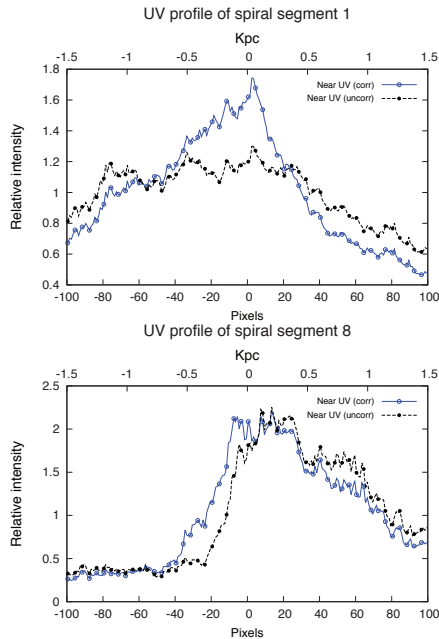


Fig. 2. Emission distributions for two segments derived from original near-ultraviolet maps and extinction corrected maps. Negative distances correspond to inner side of segments.

3. Results

Although cross sections for selected segments were derived also for HI, CO, Spitzer $3.6\mu\text{m}$, SDSS g -band and FUV emissions in next figures we compare only NIR (overall stellar mass), FIR (dust) and extinction corrected NUV emission (young stars with mean age of 10 Myr) distributions. In all cases CO and FIR distributions were quite similar. Averaged along segments emission distributions are given in Figs. 3-7.

In case of segments 1 and 11 (Fig. 3) it is very clearly seen that there is no offset between the FIR and NUV emission. Profiles of both emissions have clear peaks positions of which coincide nearly exactly. Corresponding spiral arms are quite well-defined (Fig. 1). Spiral segments 4 and 7 (Fig. 5) lie quite nearby to each other. Segment 4 was selected on the basis of NUV emission distribution, segment 7 on the basis of FIR emission. It is not clear if they form a single spiral or not. Again, no clear

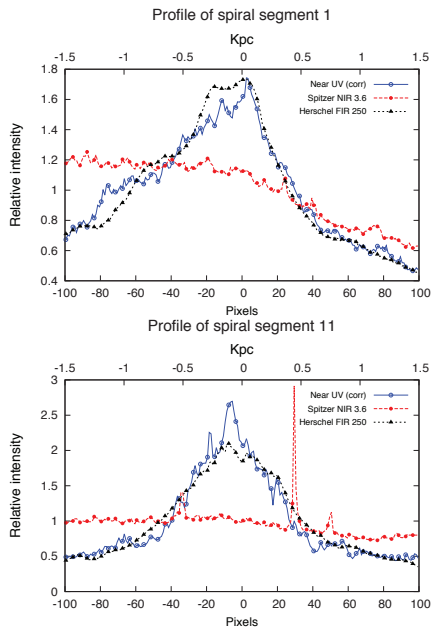


Fig. 3. Cross sections of FIR and NUV emission for segments 1 and 11. No horizontal offset between these two emission distribution are seen.

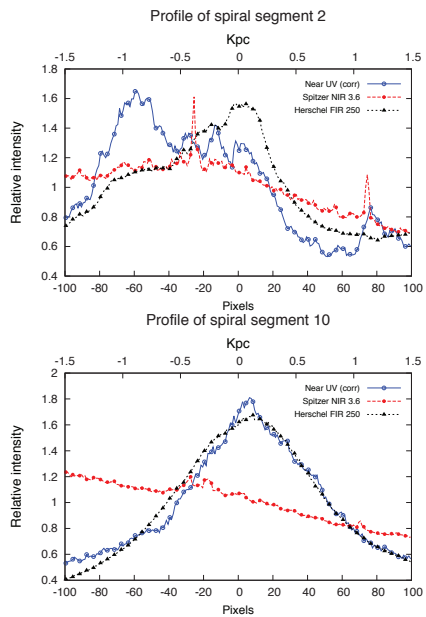


Fig. 4. Cross sections of FIR and NUV emission for segments 10 and 2.

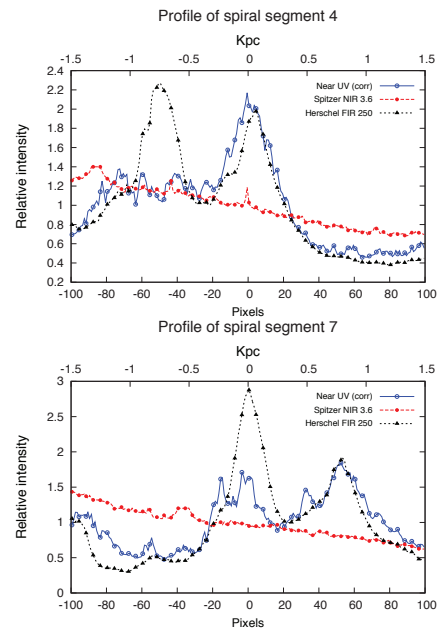


Fig. 5. Cross sections of far-IR and near-UV emission for segments 4 and 7. No clear horizontal offset between these two emission distribution are seen.

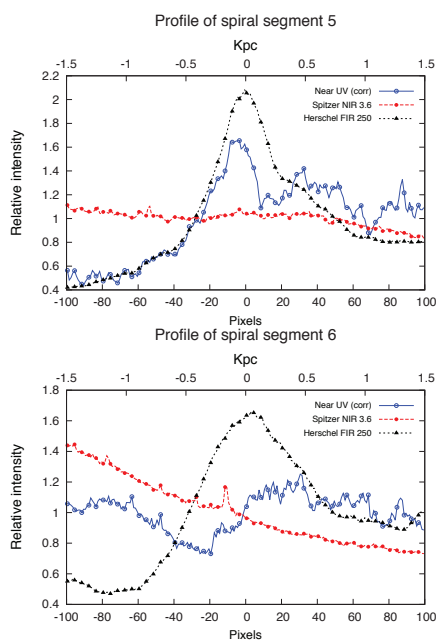


Fig. 6. Cross sections of far-IR and near-UV emission for segments 5 and 6.

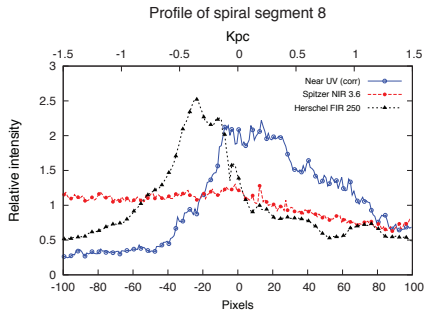


Fig. 7. Cross sections of far-IR and near-UV emissions for the segment 8, this is the only segment where an offset (300 pc) is seen.

offset is seen between FIR and NUV emission profiles. Segments 5 and 6 (Fig. 6) were both selected from FIR emission distribution. Although the spiral segment 5 is not well defined in NUV there is no offset seen for this segment. Segment 6 is not seen in NUV. The only case where a clear offset in the distribution of FIR and NUV emission cross sections is seen is segment 8 (Fig. 7). This is the shortest segment (length 3 kpc), the offset is 300 pc, dust is nearer to the center when compared to the NUV emission.

4. Conclusions

Derived FIR/CO and NUV emission cross sections along most of spiral arm segments indicate that there is no offset between star-formation tracers across the spiral arm segments. Thus, density waves are weak or absent in M 31. Our results support N-body/SPH simulations by Grand et al. (2012a,b) and D’Onghia et al. (2013) indicating that spiral arms are transient features with variable pat-

tern speeds and without significant offset between different star-forming tracers. Very weak or absent density waves were also found by Fletcher et al. (2004) that derived magnetic field orientations from radio polarization observations.

Acknowledgements. We acknowledge the financial support from the Estonian Science Foundation and the Ministry of Education and Research.

References

- Barmby, P., Ashby, M. L. N., Bianchi L. 2006, *ApJ*, 650, L45
 Corbelli, E., et al. 2010, *A&A*, 511, A89
 D’Onghia, E., Vogelsberger, M., Hernquist, L. 2013, *ApJ*, 766, 34
 Efremov, Yu. N. 2009, *Astron. Lett.*, 35, 507
 Egusa, F., Sofue, Y., Nakanishi, H. 2004, *PASJ*, 56, L45
 Fletcher, A., et al. 2004, *A&A*, 414, 53
 Fritz, J., Gentile, G., Smith, M. W. L., et al. 2012, *A&A*, 546, A34
 Gordon, K. M., Bailin, J., Engelbracht, C. W., et al. 2006, *ApJ*, 638, L87
 Grand, R. J. J., Kawata, D., Cropper, M. 2012a, *MNRAS*, 421, 1529
 Grand, R. J. J., Kawata, D., Cropper, M. 2012b, *MNRAS*, 426, 167
 Hu, T., et al. 2013, *New Astronomy*, 23, 49
 Louie, M., Koda, J., Egusa, F. 2013, *ApJ*, 763, 94
 Nieten, Ch., Neininger, N., Gulín, M., et al. 2006, *A&A*, 453, 459
 Tempel, E., Tamm, A., Tenjes, P. 2010, *A&A*, 509, A91
 Tempel, E., et al. 2011, *A&A*, 526, A155
 Thilker, D. A., Hoopes, C. G., Bianchi, L., et al. 2005, *ApJ*, 619, L67